46th AIAA/ASME/SAE/ASEE Joint Propulsion Conference & Exhibit
25 - 28 July 2010, Nashville, TN

AIAA 2010-6990

Turbine Engine Temperature Pattern Factor Control System Based on Fuel Modulation and Passive Optical Sensors

Jason Cline,[1] Jamine Lee,[2] Evan Perillo,[3] and Neil Goldstein[4]
Spectral Sciences Inc., Burlington, MA 01803

Sheree R. Swenson-Dodge,[5] John T. Ols,[6] and Stephen K. Kramer[7]
Pratt & Whitney, East Hartford, CT 06108

We present preliminary results for a new passive optical sensor that is the basis for a temperature pattern factor control system. The sensor uses the natural combustion radiance in several spectral bands to deduce the local pre-combustion equivalence ratio, which is correlated with local combustor exit temperature. The sensor was applied in an arc-sector combustor and in a closed-loop control system in a four-way laboratory burner.

Nomenclature

a	=	sensor output, giving local pre-combustion equivalence ratio from optical observation
$\mathbf{a}_0$	=	dependent-variable data at point 0
$\mathbf{A}_0$	=	matrix whose columns j correspond to the j'th element of $\mathbf{a}_0$
$\mathbf{\Delta a}$	=	matrix of row vectors, in which $\mathbf{a}_0$ has been subtracted from each row
$\mathbf{a}$	=	vector of sensed equivalence ratio pattern, from all optical observations $\{a_i\}$
$\mathbf{C}$	=	Jacobian matrix, $\partial(\mathbf{a})/\partial(\mathbf{v})$
$\tilde{\mathbf{C}}$	=	reduced-rank Jacobian matrix, $\partial(\mathbf{a})/\partial(\mathbf{v})$
F/A	=	fuel-to-air ratio, mass basis
K	=	proportional gain
M	=	number of fuel nozzles or valves
N	=	number of optical sensor stations
r	=	Euclidean distance between two points in multidimensional space
RQL	=	rich/quick-quench/lean
SLPM	=	standard liters per minute (reference condition 298 K and 1 atm)
T	=	temperature
t	=	time
β	=	intensity derivative parameter, atan2(CH′,C_2′) or atan2(CH′,OH′)
v	=	control valve setting
$\mathbf{v}$	=	vector of control valve settings
$\mathbf{v}_0$	=	independent-variable data at point 0
$\mathbf{\Delta v}$	=	matrix of row vectors, in which $\mathbf{v}_0$ has been subtracted from each row
φ	=	equivalence ratio
Δ_B	=	span of some physical quantity B, (max(B)-min(B))
σ	=	standard deviation
τ	=	characteristic time

[1] Principal Scientist, Senior Member AIAA
[2] Principal Scientist
[3] Co-op student, Northeastern University
[4] Principal Scientist and Group Leader, Spectral Diagnostics; Senior Member AIAA
[5] Hot Section Engineering-Combustors, Augmentors, and Nozzles (HSE-CAN)
[6] HSE-CAN
[7] HSE-CAN

I. Introduction

Active control of turbine engine pattern factor is a promising technology for improving performance and reducing costs of turbine engine systems. Pattern factor, which is the circumferential variation in temperature at the combustor exit, has been related to increased maintenance costs and reduced service lifetime issues. In this work we describe a generally applicable pattern factor control concept based on passive optical sensors and fuel redistribution that can be applied to a variety of turbine engines in both new and legacy aircraft.

Figure 1 shows a conceptual control system based on a distributed network of simple, engine-mounted, passive optical sensors. The sensors and fuel control valves are packaged inside a smart fuel nozzle. The valves can be used to adjust the fuel flow over a small fractional range to alleviate hot-spots in the combustor. The probes collect naturally-occurring light from the combustion zone and transmit it to a sensor that measures the relative emission intensity in a set of selected spectral bands. This ratio provides an intensity-independent indicator of the relative temperature in the sector downstream from the smart fuel nozzle. The control system compares the intensity ratios in each sector and adjusts the fuel distribution among the fuel nozzles to equalize the sensor signals while conserving the overall fuel flow to the combustor. The sensor bands used depend on the nature of the combustor. Different bands are used for rich/quick-quench/lean (RQL) combustors and premixed combustors, but the control system is the same for all combustors.

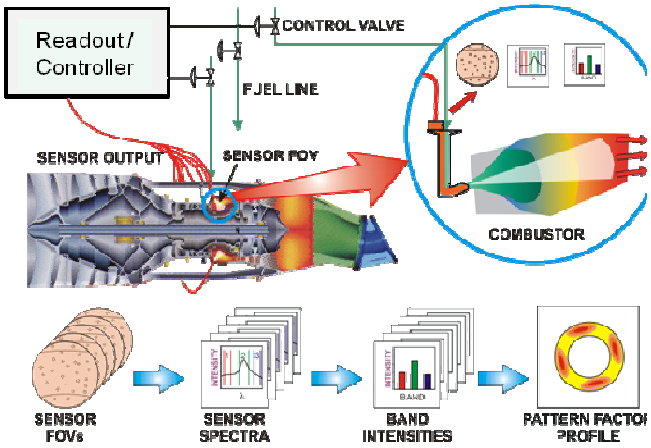

Figure 1. Concept for pattern factor control.

The control system is self-calibrating and can be used for long-term prognostics of engine performance. The system can log and maintain records of the observed band intensities as a function of operating conditions and uses a data-base of such observations to calculate the derivatives of each local sector temperature with respect to fuel flow. This establishes a matrix of variations that is used to implement a global control strategy aimed at minimizing the variation in temperature among all of the combustor segments.

The application of fuel modulation makes the system particularly robust and fault tolerant. Controlled modulation of the fuel distribution is used to measure the response of each sensor to changes in fuel flow in each burner. Thus the system measures the response of the measured temperature pattern to changes in fuel flow to each individual nozzles, which enables self-calibration and in the future may allow the control of multiple burners with a small number of redundant sensors.

In the following sections we present preliminary results for the sensor and the control system. First we report the results of optical measurements in a high-pressure RQL combustor that demonstrate the ability to measure the local equivalence ratio at the exit of the combustor using a sensor embedded in the field nozzle. We then describe the implementation of a control system for a multiple burner laboratory flame and a variety of control schemes involving an a priori calibration, self calibration based on fuel modulation, and finally control based on redundant sensors and fuel modulation.

II. Optical Sensing of Local Equivalence Ratio and Pattern Factor in an RQL Combustor

Optical emissions were measured in a high-pressure combustor using a set of passive optical sensors in an AFRL sponsored test program [Lee *et al*., 2010]. The combustor was a four nozzle sector RQL combustor designed and operated by Pratt & Whitney. A set of passive optical sensors were incorporated into the fuel nozzles. The sensors were similar to those used to monitor temperature, concentration, and equivalence ratios in high-pressure combustors [Goldstein 2002, 2003a, 2003b, 2006]. Each consists of a passive optical probe inserted into the nozzle, a fiber-optic cable to transmit the light to the readout, and a set of spectrographs that record the spectrally-resolved emission from each probe. In this case, two spectrographs were used for each nozzle, a UV/visible spectrograph operating between 250 and 480 nm, which monitors chemiluminescent emission and soot emission, and a near IR (NIR) spectrograph operating between 900 and 1600 nm, which monitors water emission. The spectra are recorded on approximately 100 Hz time scale and the data are processed to simulate the output of a simple band-pass filter centered on various spectral bands. The ratios of two bands are then used as indicators of equivalence ratio at the

exit of the combustor. A scanning extractive probe at the exit of the combustor makes an independent measure of the pattern factor of equivalence ratio at the exit, and was compared to the optical signal. Exit temperature was deduced from the well-established relationship between exit temperature and composition at the combustor exit.

Preliminary tests in a high-pressure multi-segment combustor have proven two critical properties of the control system. First, changing the fuel distribution among the various nozzles accordingly changes the exit pattern factor, as shown in Figure 2. Pattern factor was measured using a rotating array of exhaust gas samplers at the exit of the combustor. Two fuel distribution conditions are shown, balanced and unbalanced. The emission pattern downstream of the fuel nozzles directly follows the relative amount of fuel injected into each segment.

The second key result is that optical probes, located in the front end of the combustor, can track the F/A ratio in their combustor nozzle-sector. Figure 3 shows four indicators of downstream F/A measured by the optical sensor. Each is a ratio of two specific spectral bands collected by the optical sensor. Each ratio has a monotonic functional dependence on F/A over the full operating range of the combustor. Ratio A has the steepest slope at low power settings and Ratios B-D have steeper slopes for high power settings. Each of these band ratios are proportional to the segment averaged F/A ratio and the exit temperatures, and thus can be used as the input signal for the control system.

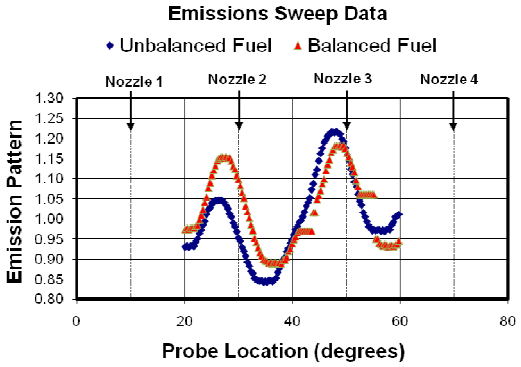

Figure 2. Pattern factor at the combustor exit for two fuel distributions.

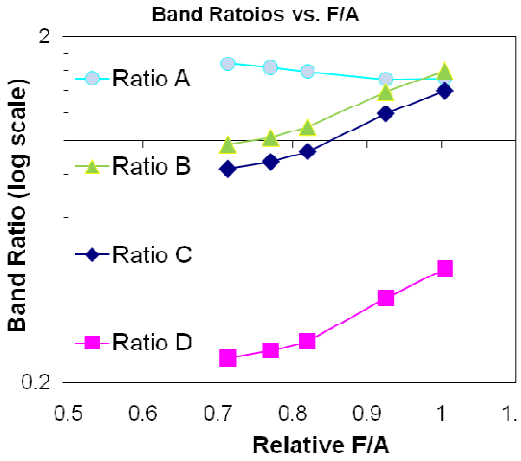

Figure 3. Band ratios vs. F/A in a high-pressure combustor.

III. Laboratory Tests of the Control System

Above we show that the sensor system produces a signal that correlates with the local F/A and can thus be used to control temperature pattern factor. In order to test the fuel-redistribution algorithm and ancillary routines in a control loop, we applied the sensor to a laboratory scale flame. The laboratory-scale combustor has four independently controllable propane/air burners. We used the same sensor readout and control concept as the high-pressure combustor but a different set of spectral bands to produce intensity ratios for use in control. Band ratios for use in control of such premixed, low-pressure combustors are well established, and include ratios of chemiluminecent emitters, such as C_2, CH, OH [Docquier 2002, Paschereit 2002, Yamaguchi 1997] and ratios of portions of the water emission band that yield a direct measurement of temperature [Goldstein 2002, 2003a, 2003b].

Figure 4 shows a schematic of the combustor, which contains four premixed ribbon burners with individually controllable fuel and air flows. The burners are arranged in a linear array, so that the 0.75-inch wide active burner surfaces spaced on 1.5" centers. The secondary air ports were not used for this work. Two combustor walls are quartz, which allows the measurement of the optical signals at the base of the flames. A set of four optical probes mounted outside the combustor collect the light radiated from the front-end of each of the burners. The probes are mounted with a view at a 30 degree angle terminating on the base of the burners. The field of view of the probes can be adjusted to control the amount of overlap between the measured sensor fields of view. In most cases, it corresponded to cone terminating in a 2-inch diameter spot centered at the surface of each burner. In other cases, the spot diameter was increased to 3 inches to allow overlap of the sensors.

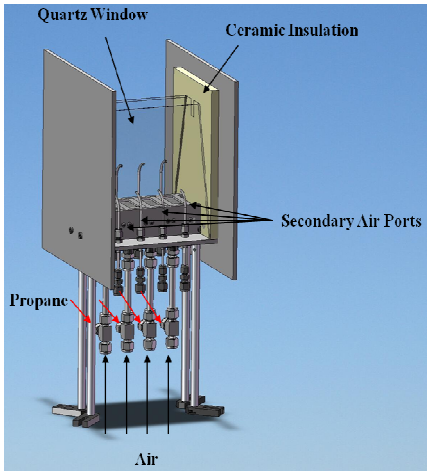

Figure 4. Schematic of burner.

The light from the probes is routed by fiber-optics to a sensor system that returns the intensity in a number of spectral bands and a set of band ratios. The sensor sends the processed data to a fuel flow controller. The controller compares the sensor data from each probe and adjusts the distribution of fuel among the burners to equalize the sensor readings. The controller can also log sensor data as a function of time, change fuel flow at each burner, generate a database of sensor output as a function of fuel flow, and compute the matrix of variation of the sensor output with respect to fuel flow among the burners. In calibration mode, the controller automatically cycles the combustor through a range of fuel distribution patterns and records the sensor response and derivatives with respect to fuel modulation.

A. Sensor Signals used for Control

Figure 5 shows some representative calibration results for two sets of sensor outputs as a function of burner equivalence ratio. The first output is the ratio of the water emission in two NIR spectral bands (wing/center) that measures the shape of 1.4 micron water band. The ratio of these bands is a direct measurement of the temperature of the water in the flow stream with an absolute temperature calibration that can be calculated from first principles without direct calibration [Goldstein *et al.* 20002, 20003]. Figure 5 also shows the water ratio data converted to temperature in this way. The right-hand figures show the ratio of C_2 and CH emission bands at 470 and 430 nm which is the primary band ratio used in the control experiments. The controller can select among these indicators, depending on the nominal operating range. The water temperature can be used for lean flames with an equivalence ratio of $\phi<0.9$ and for moderately rich flames over a range of about $1.2 <\phi<1.7$. The C_2/CH ratio can be used for $1.5<\phi$ and $\phi>1.8$. Other band ratios may be used for different nominal equivalence ratios.

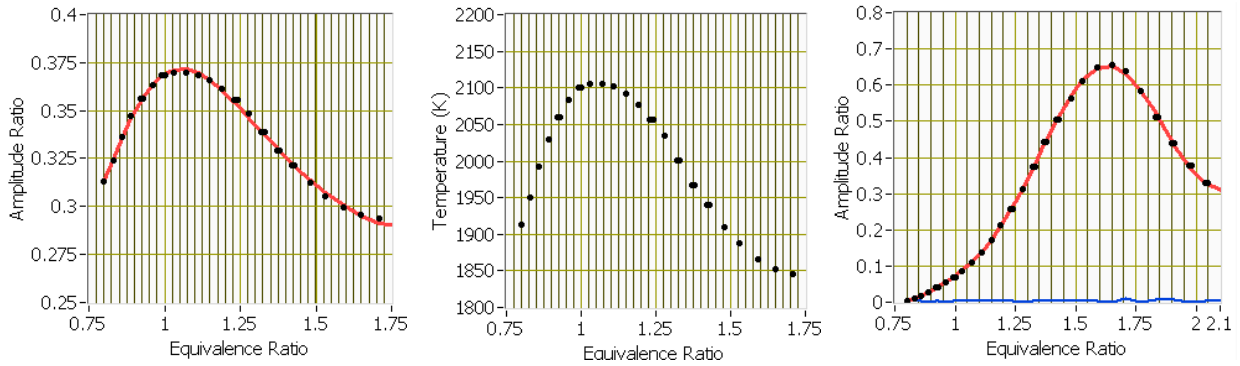

Figure 5. Sensor calibration, band ratios vs. equivalence ratio: Left – water ratio. Middle – water ratio data converted to temperature. Right – C_2/CH ratio.

We gauge the effectiveness of a sensor band ratio reading (a) for controlling local equivalence ratio by comparing its uncertainty (σ_a) to the variation of the signal with equivalence ratio ($da/d\phi$). Figure 6 illustrates how the ratio (σ_a / ($da/d\phi$)) varies with equivalence ratio. A set of sensor measurements was recorded with a one-second time constant and the standard deviation was computed at each nominal fuel and air set point. The standard deviation, σ_T, is converted to an equivalent error in the measured temperature or equivalence ratio. The one-second averaged temperature data has a one-sigma (σ_T) precision of less than 10 K, which corresponds to an equivalence-ratio precision of σ_ϕ <0.01 over most of the useable range. The C_2/CH ratio is more precise, with σ_ϕ < 0.005 over most of the useable range. Thus, while the water temperature measurement is an accurate absolute measurement of local temperature, the C_2/CH is a more precise signal for use in control. The precision of the sensor measurement is sufficient to meet the goals of reducing temperature pattern factor from the current fleet average of about Δ_T /T of about 30% to well below 10%. In fact, the precision of the C_2/CH would propagate to an error band of less than $\Delta_\phi<0.02$ or Δ_T <5K, and would use up less than 5% of the overall control system error budget.

The sensor measures in several bands simultaneously, and thus has several band ratio outputs available at any given time. By intelligently selecting from the available presets, we have a reliable basis for a control signal over a range of F/A ratios.

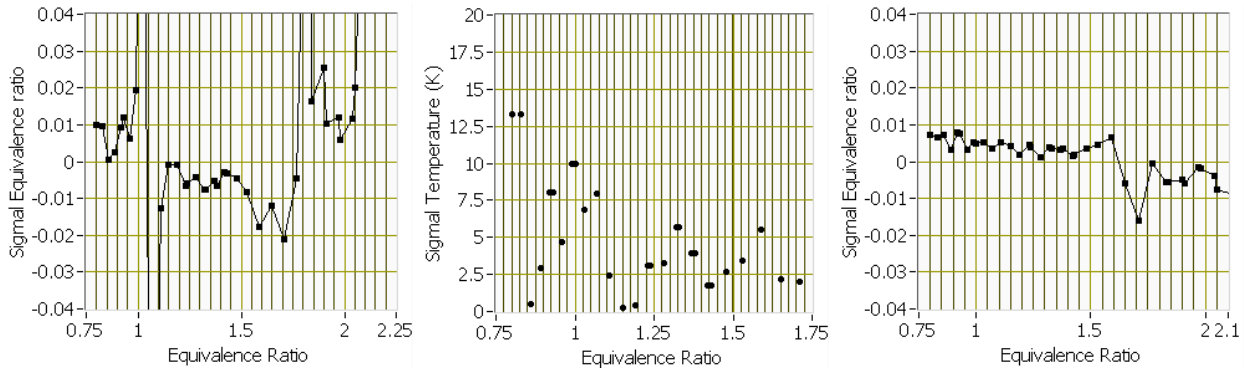

Figure 6. Sensor error propagation relative to sensitivity: Left–$\sigma_\phi/(da/d\phi)$ based on water band ratio. Middle–measured temperature error, $\sigma_T/(dT/d\phi)$, based on water ratio. Right–$\sigma_\phi/(da/d\phi)$ based on C_2/CH ratio.

B. Basic Control Concept

The control system measures differences among the sensor signals and responds by diverting fuel from burners with high ϕ to the other burners to reduce the pattern factor. The system measures the pattern factor based on the combination of sensor signals and estimates the change in fuel distribution required to equalize the sensor readings subject to the constraint that total fuel flow is constant. The controller then periodically outputs updated valve settings that provide an incremental step towards zero pattern factor.

The control system can be implemented with a variety of sensor inputs and calibration functions. The simplest approach uses the value of band ratios measured in each combustor segment, and an estimated scalar derivative of the sensor output with respect to equivalence ratio. The system is overdamped to make it relatively insensitive to the initial estimate of the derivative. It converges to the condition of equal sensor signals provided the controller is sufficiently damped and the sign of the derivative is correct. At the next level of sophistication, the derivatives of the sensor with respect to fuel flow can be measured using an automated calibration procedure, and a matrix of variations used to provide a more accurate estimate of the path to equal sensor response. Finally, the system can use the response of a common sensor, or group of sensors to fuel modulation as the basis of the control signal.

The controller compares the sensor signals from the four burner segments, and computes, Δa_i the deviation of sensor reading a_i from the mean reading of all sensors. The algorithm computes the changes in fuel valve settings, Δv_i, for each nozzle j that will bring the system closer to equilibrium. This is done through simultaneously solving N linear equations, indexed in i, of the form

$$-\Delta a_i = \sum_j \left(\frac{\partial a_i}{\partial v_j}\right) \Delta v_j \tag{1}$$

where $(\partial a_i/\partial v_j)$ is the partial derivative of the signal at sensor i with respect to a change in fuel flow at valve j, while holding all other valve settings fixed. In matrix notation, this is

$$\Delta \mathrm{a} = \mathrm{C}\, \Delta \mathrm{v} \tag{2}$$

where $\mathbf{C}$ is the Jacobian matrix. The resulting valve change vector $\Delta\mathbf{v}$ is the one that produces changes in $\{a_i\}$ such that the resulting set of sensor returns is uniform.

As mentioned above, one of our objectives is to reduce pattern factor without changing overall fuel consumption rate. Therefore the total fuel flow is constrained to be constant at a given operating point. This adds a constraint that all changes must sum to zero. This constraint can be applied directly in the $\mathbf{C}$ matrix, reducing it from M to $(M-1)$ columns.

$$\tilde{\mathrm{C}} = \begin{pmatrix} (\mathrm{c}_{1,1} - \mathrm{c}_{1,\mathrm{M}}) & (\mathrm{c}_{1,2} - \mathrm{c}_{1,\mathrm{M}}) & \cdots & (\mathrm{c}_{1,\mathrm{M}-1} - \mathrm{c}_{1,\mathrm{M}}) \\ (\mathrm{c}_{2,1} - \mathrm{c}_{2,\mathrm{M}}) & (\mathrm{c}_{2,2} - \mathrm{c}_{2,\mathrm{M}}) & \cdots & (\mathrm{c}_{2,\mathrm{M}-1} - \mathrm{c}_{2,\mathrm{M}}) \\ \vdots & & \ddots & \vdots \\ (\mathrm{c}_{\mathrm{N},1} - \mathrm{c}_{\mathrm{N},\mathrm{M}}) & (\mathrm{c}_{\mathrm{N},2} - \mathrm{c}_{\mathrm{N},\mathrm{M}}) & \cdots & (\mathrm{c}_{\mathrm{N},\mathrm{M}-1} - \mathrm{c}_{\mathrm{N},\mathrm{M}}) \end{pmatrix} \tag{3}$$

By providing $\tilde{\mathbf{C}}$ and $\Delta\mathbf{a}$ we can then solve for the recommended change in valve state, $\Delta\mathbf{v}$.

$$\tilde{\mathrm{C}}\begin{pmatrix}\Delta \mathrm{v}_1\\ \Delta \mathrm{v}_2\\ \vdots\\ \Delta \mathrm{v}_{\mathrm{M}-1}\end{pmatrix}=\begin{pmatrix}\Delta \mathrm{a}_1\\ \Delta \mathrm{a}_2\\ \vdots\\ \Delta \mathrm{a}_{\mathrm{N}}\end{pmatrix} \tag{4}$$

We provide $\Delta\mathbf{a}$ and solve for $\Delta\mathbf{v}$ using standard methods, such as those in LAPACK DGELS() [Anderson *et al*., 1999] (or analogous routine). The value of Δv_M is defined by the fuel flow constraint.

The calculation estimates a valve change vector $\Delta\mathbf{v}$ that will minimize the pattern factor. This vector is multiplied by a fractional step size K to dampen the action, in anticipation that the true behavior is only locally linear. The control loop updates every Δt seconds, where Δt is adjustable. Were the optimal solution to lie close to the original position, such that all systems were behaving in a strictly linear way, then the system approaches equilibrium with a characteristic time constant, τ, given by:

$$\tau_{\mathrm{calc}} = \frac{\Delta t}{\ln \frac{1}{1-K}} \tag{5}$$

If the final value of $(\partial a_i/\partial v_j)$ is different from the initial estimate, the system converges with a different observed time constant, τ_{obs}, provided K is sufficiently small.

C. Control using *a priori* Scalar Calibration

In its initial implementation, the Jacobian matrix of $(\partial a_i/\partial v_j)$ values is replaced with a diagonal matrix whose diagonal elements are all the samemaking it effectively scalar. These derivatives were based on an *a priori* estimate of sensor response based on the response curves shown in Figure 5. Figure 8 shows the response of the system under closed loop control with an overall equivalence ratio of ϕ=1.25 and an air flow of 18 SLPM. The system starts with nominally equal air flow to all burners, and a fuel distribution that keeps the sensor signals equal in all the burners. The fuel distribution among the burners varies by a few percent, which counteracts the effects of uneven air distribution within the combustor. At time t=0, the air flow is decreased to burner #2 by –5.6%, with concomitant increases to the other burners of +1.9%. The control system responds to bring the sensors back into equilibrium, resulting in a fractional fuel change of –5.5% in burner #2.

Figure 8 plots the time history of the air flow, the sensor signals, the fuel flow, and the observed flame-base water temperature for each of the two central burners. This data was collected with a damping constant, K, chosen to be about 1/3 of that which produces sustained oscillation. The observed decay time of τ_{obs}=9.2 s is close to the initial estimate of τ_{calc} = 9.7 s, indicating a good initial estimate for $(\partial a_i/\partial v_j)$. Figure 9 shows the results when the damping coefficient is chosen to send the system into sustained oscillation.

The performance of the control system is summarized numerically in Table 1. At steady state, the fuel flow to each burner is held steady with a fractional rms AC error of just under 0.1%, which is approximately equal to the variation in the air flow. This is consistent with the observed variation in the sensor signal, of about 1% $(\mathrm{Hz})^{-1/2}$ rms, given the longer averaging time (τ=10s vs. the 1s averaging time for the sensor), and the transfer function of $(\mathrm{d}\phi/\mathrm{d}a)/(\phi/a)$=1/3. The response of the system to increased air results in an equal increase in fuel (within an error of ± 0.1%), indicating that the measured C_2/CH ratio is a good indicator of local F/A and results in stable control of F/A at each burner. In short, the control system maintains the F/A ratio within a control band of ±0.2 % including both AC and DC errors.

In contrast, the temperature measured by the water band ratio has substantial random and periodic variations, that reflect flickering of the flame and other time-dependent variations in the flame exhaust pattern. This is due to the fact that the water temperature and the C_2/CH ratio measure different parts of the flame: the C_2/CH ratio emphasizes the active flame region close to the burner, while the water emission comes from the flame exhaust. The control system was set up to view a 2" diameter cone at the base of the flame, which contains nearly all the C_2 and CH emission. The water emission generally comes from higher up in the flame, and the water signals vary with time as the flame height changes.

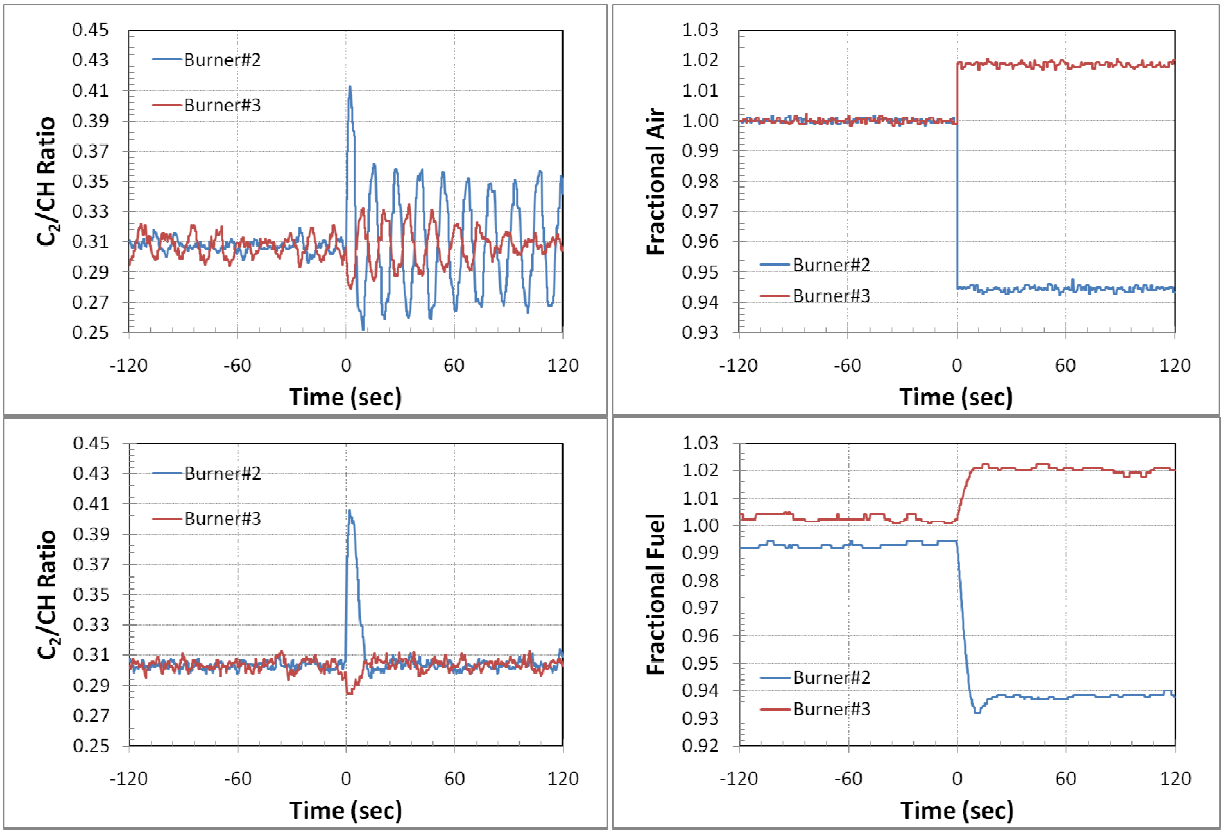

Figure 8. Damped control system with *K*=0.02. Top left: Air distribution, Top right: Sensor response (1 s time constant), Bottom Left: Fuel flow, Bottom right: Temperature based on water ratio (1s time constant).

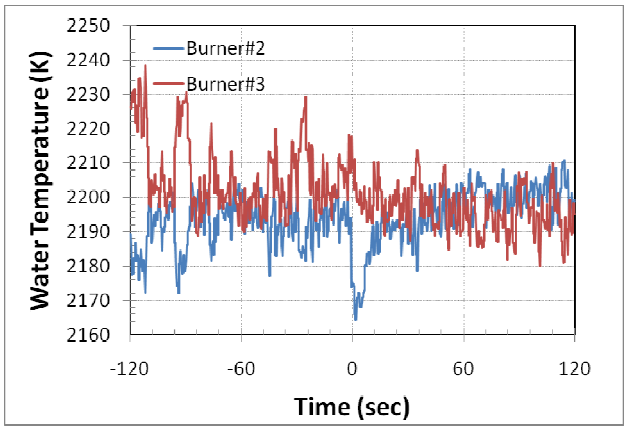

Figure 9. Stable oscillation with a *K*=0.067 and a period of 13 seconds.

Table 1. Performance parameters for the control system.

Condition	Time Response			RMS AC				Step Change		Response
	K (%)	τ_{calc} (s)	τ_{obs} (s)	Air %	Fuel %	Sensor %	Water T (K)	Δ Air, Burner 2	Δ T, Burner 2	Δ Fuel, Burner 2
Damped	2.0	9.6	9.2	0.08%	0.09%	0.95%	5.6	5.56%	20 K	5.53%
Oscillatory	6.0	2.9	2.1	0.07%	2.18%	10.72%	12.2	5.58%	25K	5.67%

D. Control with a Vector Derivative and Self-calibration

In the next level of complexity, the Jacobian matrix would be fully populated so that variations from adjacent burners (where $|i–j|=1$ or more) are taken into account. We chose to demonstrate the self-calibration feature by initializing the Jacobian from experimental data where there is definite field-of-view overlap and where a specific pattern is cycled among the valves. We have not yet had the opportunity to use the vector derivative in closed loop control.

To obtain the data experimentally, we pointed and focussed our sensor fields of view to a 3-inch spot on their respective burner surfaces. Because the burners are spaced on 1.5" centers, there is significant spatial overlap. We recorded sensor returns (C_2/CH band ratios) for our flame system in a series of conditions wherein the air to one burner was different than the other three, cycling an equivalence ratio pattern of (+ – – –) among the burners, as well as one nominal condition in which $\varphi=1.25$ on all burners. Figure 10 shows the results plotted in aggregate. As with the function measured when all burner equivalence ratios are the same (Figure 5), the intensity returned is not linear in φ, changing slope somewhere between φ values of 1.40 and 1.55. The data have scatter, because of different signal magnitudes between burners and/or sensors, deviation of the true equivalence ratio from the nominal value due to mixing and combustor irregularities, and also because of covariance between adjacent burners: every sensor sees a portion of the flow from adjacent burner zones.

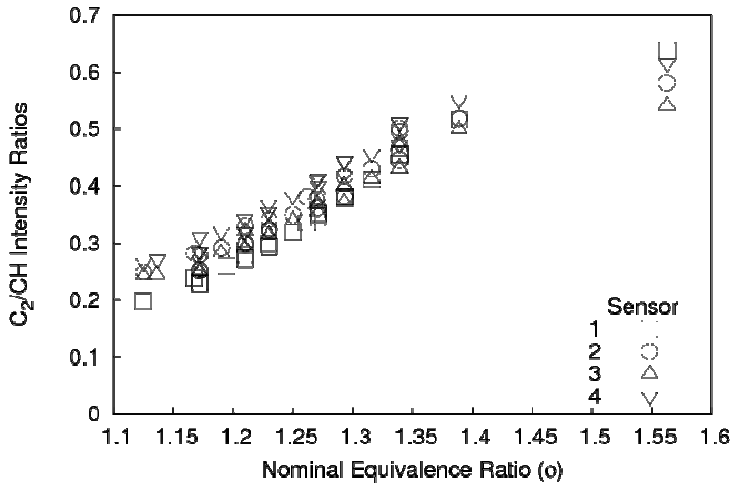

Figure 10. Sensor output versus nominal equivalence ratio. Data from all sensors is shown.

In an operational system, the control system would use a calibration function that is specific to the nominal operating conditions. For any nominal condition, the calibration function would be expressed in the form of a Jacobian matrix centered on the nominal fuel condition. The Jacobian is calculated from a database of calibration measurements, such as those in Figure 10. In this work, we calculated the Jacobian matrix centered at $\varphi=1.25$ using two methods: a linear fit, and a linearized second-order fit. We then tested the results in terms of how well the Jacobian could reproduce the training data set based on multidimensional linear extrapolation from a query point.

The first result is that for a linear fit using all the data of Figure 10. The Jacobian was first fit to all of the data simultaneously using a minimum-norm solution to the equation

$$\Delta v \cdot C = \Delta a \tag{6}$$

Figure 11 shows the correlation between prediction and data. It is clear that the nonlinear portion of the data is affecting the quality of the fit.

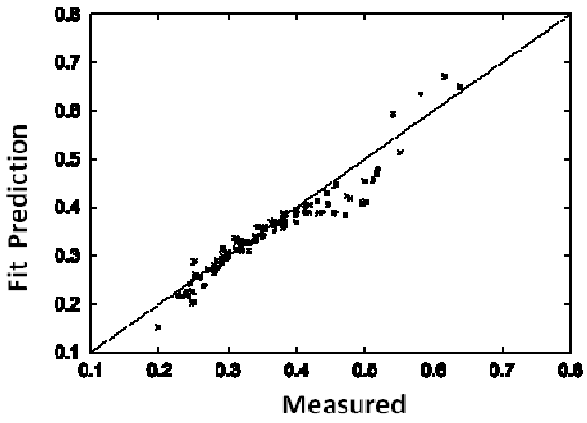

Figure 11. Correlation plot of linear multidimensional fit to all data in Figure 10.

The second result is that for a constrained second-order fit. The flame data have a global nonlinearity that degrades local linear fits. The fit can be significantly improved by fitting the data local to the query point with a quadratic model, then using only the linearized slope function for the Jacobian. Locality was imposed by an inverse-distance weighting function of $\exp(-5r^2)$, where r is the distance between the query point and the data point in the scaled coordinate space of the data. Figure 12 shows the performance of this Jacobian. There are still outliers, but the majority of the data are now well-predicted.

Some care is warranted with this type of fit, because when there are not enough data in each coordinate direction, the second-order coefficients, left unconstrained, can dominate the fit and produce nonsensical first-order results. Additionally, good results rely on a proper specification of the quadratic lengthscale for the weighting—while performance thus far has been generally insensitive to them when properly specified, grossly erroneous lengthscales yield poor predictions. We anticipate that the above caveats can be heeded with simple heuristics, and that this type of parameterization will be performed for a variety of burner operating points.

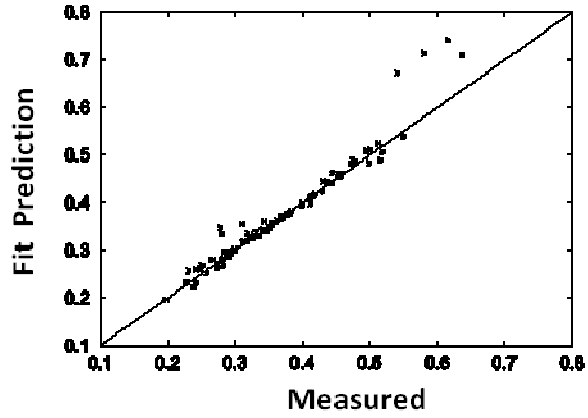

Figure 12. Correlation plot for the constrained second-order fit to all data in Figure 10. The result is based on a query location of $\boldsymbol{\phi_1 = \phi_2 = \phi_3 = \phi_4 = 1.25}$.

In this section, we have shown that we can improve the controller's optimization solution by fitting all of the coefficients of the Jacobian matrix. This in turn increases the stability of the control by providing a larger gain margin. The improvement using the constrained linearized second-order fit is substantial and will increase convergence rate of the burner system to an even temperature pattern.

E. Fuel Modulation and Derivative Control

Until now we have been discussing control using the uniformity among ratios of in-band intensities at several burner-sectors as the control variable. But perhaps the most exciting aspect of this control technology is the potential to use not ratios of intensities, but, by using fuel modulation, to measure and use fuel-flow *derivatives* of intensities as the basis for control. As we will explain below, this alternative type of control signal measurement could potentially reduce the number of sensors per engine to one.

For intensity signals that are nonlinear with respect to temperature or exit-plane local equivalence ratio, we can exploit the nonlinearity in a way that dramatically increases the robustness of the control-variable measurement. By continually modulating the fuel distribution among known patterns, we can measure the intensity derivatives for each sensor/valve combination. But because the measurement depends entirely on ratios of differences, having one sensor per burner would excessively overspecify the Jacobian. In this scheme, as long as light from every burner-sector is observed, the Jacobian is uniquely determined. This can dramatically reduce the number of sensors required for complete and redundant coverage of an engine. If light from all sectors of the engine can be seen by a single sensor, then this is sufficient for control using ratios of fuel-flow derivatives.

Experimental data from our laboratory system show that the φ-derivatives in selected bands vary in a way that maps φ while remaining insensitive to operating condition. Figure 13 shows the experimentally-derived mapping of intensity derivative ratios as a function of equivalence ratio.

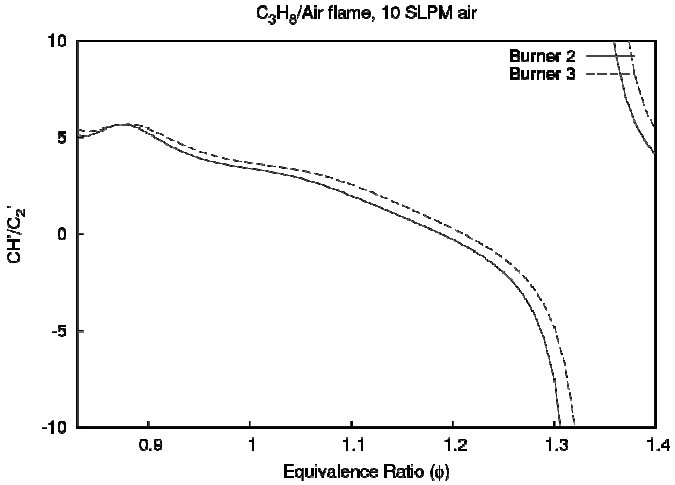

Figure 13. Ratio of φ-derivatives of CH and C_2 intensities in the laboratory flame at 10 SLPM air and a range of equivalence ratios.

Figure 14 is a parametric plot of the φ-derivative of the intensity in two sensor bands, obtained by fitting a polynomial in φ to the data from each sensor and condition, then differentiating analytically. Data for four sensors and six air-flow settings are shown. The air flow settings are 10, 12, 14, 16, 18, and 20 SLPM air. Despite the factor of two range in air flow, the parametric plot shows a pattern in the equivalence ratio, suggesting a kind of phase angle between the intensity curves when plotted against equivalence ratio.

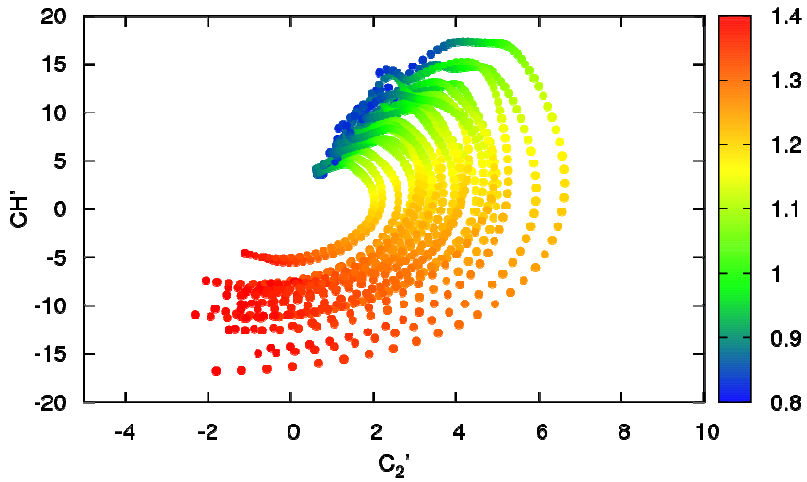

Figure 14. Change in φ with pairs of φ-derivatives of two in-band intensities, for a range of $0.83 < \phi < 1.4$. The color bar is φ equivalence ratio.

In Figure 15 we plot that angle; the figure shows a mapping between this angle and equivalence ratio φ for two sets of intensity bands, C_2'/CH', and OH'/CH'. To avoid singularities at zero-crossings, we have parameterized the data in terms of its angle β in the parametric intensity space of Figure 14, where β is the angle formed by a data point, the origin as the vertex, and point (1,0). The data form bands because they are derived from four views at six different conditions, but the general trends are clear - the angle β maps closely to equivalence ratio for each band pair. This confirms that the derivative ratio is principally sensitive to equivalence ratio, and far less sensitive to the peculiarities of condition changes (e.g., total flow rate) and sensor.

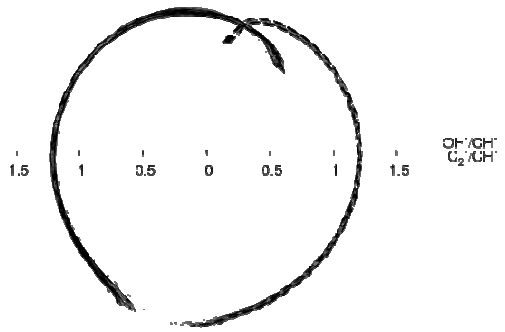

Figure 15. Polar plot of equivalence ratio as a function of angle β, for two pairs of bands. The data was analyzed in the range of $0.83 < \phi < 1.4$. Radius is equivalence ratio.

The extra cost of using fuel flow modulation to measure the derivatives is offset by the additional capabilities that this protocol provides. The first, and simplest benefit, is that any measurement offsets are eliminated. The intensity offsets tend not to vary with fuel flow, or vary slowly, and therefore vanish in the derivative. This potentially eliminates interference from hot metal parts whose emission responds more slowly to fuel changes than the combustion flow.

Another benefit is fault-tolerance. In the former direct-intensity method, when the number of measurements is less than the number of burner-sectors, it is difficult or impossible to identify the fraction of intensity from a given light source without some *a priori* calibration. In the derivative-ratio concept, were a sensor to fail, sensors whose fields of view overlap that of the failed sensor can provide readings.

Perhaps the greatest benefit is the opportunity to reduce the number of sensors to a number much smaller than the number of valves. A small number of sensors with overlapping fields of view can be used along with fuel modulation to provide complete and redundant pattern factor measurement.

IV. Conclusion

We have demonstrated two necessary conditions for control of pattern factor using optical sensors located in the fuel nozzle of RQL combustors: 1) the optical sensors track fuel/air ratio at the exit of the combustor, and 2) modulation of fuel at the fuel nozzle controls the equivalence ratio at the exit. We have also demonstrated in the laboratory a control system based on equalizing the sensor signals from various segments of the combustor using fuel control. This system is consistent with an engine operation, in which the total fuel flow is conserved, but fuel is redistributed to minimize pattern factor. We have shown that the controller can be initialized from a database of measurements, where those measurements could be acquired in-flight. Finally we introduce a sensor concept wherein the outputs are the fuel-flow-derivatives of the measurements. This concept requires continual fuel-flow modulation and tight integration between the sensor and controller but provides benefits of increased measurement robustness and a high degree of fault tolerance.

Acknowledgments

The authors thank J. Scott Kearney of United technologies Research Center, Urmila Reddy of Pratt & Whitney, and Philip Lee and Marc Paskin of Woodward Fuel Systems Technology for their dedicated efforts in preparing for and conducting the high pressure tests, and Alexander Turovsky of Northeastern University for his assistance in performing the laboratory tests of the control system. The authors also thank Kenneth Semega of AFRL/RZTF and

Carlos Arana of AFRL/RZTC for technical guidance. This work supported by an AFRL SBIR contract No. FA8650-07-C-2730.

References

Anderson, E., Z. Bai, C. Bischof, S. Blackford, J. Demmel, J. Dongarra, J. Du Croz, A. Greenbaum, S. Hammarling, A. McKenney, and D. Sorensen, "LAPACK Users' Guide," 3rd Edition, *Society for Industrial and Applied Mathematics*, Philadelphia, PA, 1999.

Docquier, N. and S. Candel, "Combustion control and sensors: a review," Progress in Energy and Combustion Science 28:107, 2002.

Goldstein, N., C.A. Arana, F. Bien, J. Lee, J, Gruninger, T. Anderson, W.M. Glasheen, "Innovative Minimally Intrusive Sensor Technology Development for Versatile Affordable Advanced Turbine Engine Combustors," *Proceedings of the ASME Turbo Expo, 2002*, GT-2—2300051, 2002.

Goldstein, N., Adler-Golden, S.M., Jin, X., Richtsmeier, S.C., Lee, J., and Arana, C.A., "Temperature and Temperature Profile Measurements in the Combustor Flowpath using Structured Emission Thermography," *Proceedings of the ASME Turbo Expo, 2003*,GT2003-38695, 2003a.

Goldstein, N., Gruninger, J.H., Bien, F., Lee, J., US patent application for a "System and Method for Optically Determining Properties of Hot Fluids from the Spectral Structure of Emitted Radiation," Patent Docket No. US6640199, 2003b.

Goldstein, N., Jin, X., Gregor, B., Lee, J., Kramer, S. K., Kozola, S., Semega, K. J., "IR Structured Emission-based Speciation, Thermometry, and Tomography of CO and H2O in High-Pressure Combustors," *Proceedings of the ASME Turbo Expo, 2006*, 2006.

Lee, J., J. Cline, and N. Goldstein, "Pattern Factor Control Based on Fuel Modulation and Passive Optical Sensors," Phase II Final Report, under Phase II Contract No. FA8650-07-C-2730, SSI Technical Report TR-563, Spectral Sciences Inc., Burlington, MA, 2010.

Paschereit, C.O. and Gutmark, E., "Proportional Control of Combustion Instabilities in a Simulated Gas-Turbine Combustor," *Journal of Propulsion and Power*, Vol. 18, No. 6, 2002.

Yamaguchi, T., K.T.V. Grattan, H. Uchiyama, and T. Yamada, "A practical fiber optic air-ratio sensor operating by flame color detection," *Review of Scientific Instruments*, 68(1): 197, 1997.